CERS2 Suppresses Tumor Cell Invasion and is Associated with Decreased V-ATPase and MMP-2/MMP-9 Activities in Breast Cancer

Shao-hua Fan,[1] Yan-yan Wang,[2] Jun Lu,[1] Yuan-lin Zheng,[1]* Dong-mei Wu,[1] Zi-feng Zhang,[1] Qun Shan,[1] Bin Hu,[1] Meng-qiu Li,[1] and Wei Cheng[3]

[1]Key Laboratory for Biotechnology on Medicinal Plants of Jiangsu Province, School of Life Science, Jiangsu Normal University, Xuzhou, Jiangsu 221116, China

[2]Department of Function Examination, The First People's Hospital of Xuzhou, Xuzhou, Jiangsu 221000, China

[3]School of Environment and Spatial Informatics, China University of Mining and Technology, Xuzhou, Jiangsu 221008, China

ABSTRACT

Ceramide synthase 2 (CERS2) is the gene identified from a human liver cDNA library in 2001. Our previous studies have shown higher expression of CERS2 in the breast cancer patients was associated with fewer lymph node metastases. However, the molecular mechanism of CERS2 involved is unknown. Here, we found CERS2 was heterogeneously expressed in various breast cancer cells. The mRNA and protein expression levels of CERS2 in MCF7 cells, which are poorly invasive breast cancer cells, were obviously higher than that in the highly invasive cells MDA-MB-231. Results showed overexpression of CERS2 in MDA-MB-231 cells could significantly inhibit the migration and invasion ability, whereas CERS2 knockdown in MCF7 cells could significantly increase the migration and invasion ability. Overexpression of CERS2 in MDA-MB-231 cells significantly reduced the V-ATPase activity, increased the extracellular pH and decreased the pH-dependent activity of MMP-2 and MMP-9 matrix metalloproteinases (MMPs). CERS2 knockdown in MCF7 cells significantly increased the V-ATPase activity, decreased the extracellular pH and increased the activity of MMP-2 and MMP-9. Taken together, CERS2 can significantly inhibit breast cancer cell invasion and is associated with the decrease of the V-ATPase activity and extracellular hydrogen ion concentration, and in turn the activation of secreted MMP-2/MMP-9 and degradation of extracellular matrix (ECM), which ultimately suppressed tumor's invasion. Thus, CERS2 may represent a novel target for selectively disrupting V-ATPase activity and the invasive potential of cancer cells. J. Cell. Biochem. 116: 502–513, 2015.   © 2014 Wiley Periodicals, Inc.

KEY WORDS: CERS2; BREAST CANCER; INVASION; V-ATPASE

Breast cancer is the most frequent malignancy in women and the second-leading cause of cancer-related deaths [Siegel et al., 2013]. The lethal outcome of the vast majority of breast cancer is due to the dissemination of metastatic tumor cells and

the outgrowth of secondary tumors at distant site. The initiation of metastasis involves the invasion of the tumor into the peripheral tissue leading to intravasation of cancer cells into blood or lymphatic vessels from where they disseminate into secondary organs [Kessenbrock et al., 2010]. Invasion requires the crossing of several physical barriers, such as extracellular matrix (ECM) (Cardoso et al., 2014; Fang et al., 2013). The ECM maintains tissue polarity and architecture and prevents cancer cell invasion [Lu et al., 2012].

The vacuolar-H^+-ATPase (V-ATPase) is an important pH regulatory complex in tumor cells and positively correlated to cancer invasion and metastasis, it is required to mediate signaling pathways, such as the Wnt pathway [Rojas et al., 2006; Cruciat et al., 2010]. V-ATPase uses the energy produced by ATP hydrolysis to pump protons into the extracellular environment. The low pH of tumor extracellular microenvironment may induce the increased secretion and activation of degradative enzymes, such as matrix metalloproteinases (MMPs). Moreover, low extracellular pH may promote the degradation and remolding of ECM through proteolytic enzyme activation, thus contributing to cancer invasion and metastasis [Rofstad et al., 2006; Fais et al., 2007]. V-ATPases are overexpressed in many types of metastatic cancers and positively correlated to their invasion and metastasis [Fais et al., 2007]. In breast cancer cells, the abundance of V-ATPase on the plasma membrane correlates with an invasive phenotype [Chung et al., 2011]. Furthermore, V-ATPase inhibitors reduce cell migration in cancer cells with high levels of plasma membrane V-ATPase [Sennoune et al., 2004; Wiedmann et al., 2012]. There is evidence that the inhibition of V-ATPase function via knockdown of *ATP6V0C* (ATPase, H^+ transporting, lysosomal 16 kDa, V0 subunit c) [ATP6V0C is also designated as ATP6L (16 kDa subunit of proton pump V-ATPase) or VPL (proteolipid subunit of vacuolar H^+ ATPase)] expression using RNA interference technology could effectively suppress cancer metastasis by the decrease of proton extrusion and the down-regulation of protease activity [Lu et al., 2005].

Ceramide synthase 2 (*CERS2*), which is also called *LASS2* (*Homo sapiens* longevity assurance homolog 2 of yeast LAG1) or *TMSG1* (tumor metastasis suppressor gene), is the gene identified from a human liver cDNA library and interacts with VPL [Pan et al., 2001]. *CERS2* is one member of *CERS* family, including *CERS*1–6 [Laviad et al., 2008]. Recently, it has been reported that total ceramide levels in malignant breast tumors were statistically significantly elevated when compared with normal tissue samples [Schiffmann et al., 2009]. The augmentation of the various ceramides could be assigned to an increase of the messenger RNA levels of *CERS2*, *CERS4* and *CERS6* [Schiffmann et al., 2009; Erez-Roman et al., 2010]. Notably, elevated levels of $C_{16:0}$-Cer were associated with a positive lymph node status [Schiffmann et al., 2009]. Some researchers found an increased expression of CERS5 in 50% of investigated colorectal carcinomas, which was associated with lymphovascular invasion, metastasis and poor survival in colorectal cancer patients [Fitzgerald et al., 2013]. Some researchers detected decreased CERS1 expression in human head and neck squamous cell carcinomas. In contrast, overexpression of CERS1 in head and neck squamous cell carcinomas cells leads to an inhibition of cell

proliferation [Koybasi et al., 2004; Schiffmann et al., 2009]. Our previous studies have shown that CERS2 was involved in chemotherapeutic outcomes and low CERS2 expression may predict chemoresistance [Fan et al., 2013]. In addition, we also found higher expression of CERS2 in the breast cancer patients was associated with fewer lymph node metastases [Wang et al., 2013], however, the molecular mechanism of CERS2 involved is unknown. In this study, we found CERS2 expression was markedly different between various breast cancer cells and correlated inversely with invasion activity of cells, then further elucidated the molecular mechanism of *CERS2* involved in invasion.

MATERIALS AND METHODS

CELL LINES
Human breast cancer cell lines, T-47D, SK-BR-3, MDA-MB-468, MDA-MB-453, MDA-MB-231, and MCF7, were purchased from the American Type Culture Collection (ATCC, Manassas, VA). Human breast cancer cell line Bcap-37 was purchased from the Committee on Type Culture Collection of Chinese Academy of Sciences (Shanghai, China).

VECTOR CONSTRUCTS
The *CERS2* lentivirus expression vector pWPXL-*CERS2* was constructed by replacing the green fluorescence protein fragment of the pWPXL vector (Addgene plasmid 12257, Didier Trono) with the coding sequence of *CERS2* (NM_181746) amplified from the human liver cDNA library. The primers used are as follows: 5′-TATACGCGTATGCTCCAGACCT TGTA-3′ (L) and 5′-GCTACTAGTT-CAGTCA TTCTTACGATGGT-3′ (R).

Oligonucleotides were synthesized to generate an annealing shRNA targeting the sequence of *CERS2* from position 764 to 782 (5′-GGCCCAGTCTCCTCAAGAA-3′, shRNA1-*CERS2*) or from 923 to 941 (5′-AGTATTGGTACTACATGAT-3′, shRNA2-*CERS2*). The fragments were cloned separately into pLVTHM (Addgene plasmid 12247, Didier Trono) using the restriction sites *Mlu*I and *Cla*I. The sequences used are as follows: shRNA-vector, 5′-CGCGTCCCCTTCTCCGAACGTGTCAC-GTTTCAAGAGAACGTGACACGTTCGGAGAATTTTTGGAAAT-3′ (L), 5′-CGATTTCCAAAAATTCTCCGAACGTGTCACGTTCTCTTGAAACG-TGACACGTTCGGAGAAGGGGA-3′ (R); shRNA1-*CERS2*, 5′-CGC-GTCCCCGGCCCAGTCTCCTCAAGAATTCAAGAGATTCTTGAGGAG-ACTGGGCCTTTTTGGAAAT-3′ (L), 5′-CGATTTCCAAAAAGGCCCA-GTCTCCTCAAGAATCTCTTGAATTCTTGAGGAGACTGGGCCGGGG-A-3′ (R); shRNA2-*CERS2*, 5′-CGCGTCCCCAGTATTGGTACTACAT-GATTTCAAGAGAATCATGTAGTACCAATACTTTTTTGGAAAT-3′ (L), 5′-CGATTTCCAAAAAAGTATTGGTACTACATGATTCTCTTGAAAT-CATGTAGTACCAATACTGGGGA-3′ (R).

Oligonucleotides were synthesized to generate an annealing shRNA targeting the sequence of *ATP6V0C* from position 574 to 592 (5′-TCGGCCTCTACGGTCTCAT-3′, shRNA1-*ATP6V0C*) or from 314 to 332 (5′-GTCCATCATCCCAGTGGTC-3′, shRNA2- *ATP6V0C*). The fragments were cloned separately into pLVTHM (Addgene plasmid 12247, Didier Trono) using the restriction sites *Mlu*I and *Cla*I. The sequences used are as follows: shRNA1-*ATP6V0C*, 5′-CGCGT-CCCCTCGGCCTCTACGGTCTC

ATTTCAAGAGAATGAGACCGTAGAGGCCGATTTTTGGAAAT-3′(L), 5′-CGATTT CCAAAAATCGGCCTCTAC- GGTCTCATTCTCTTGAAAT-GAGACCGTAGAGGCCGAGGGGA-3′ (R); shRNA2-*ATP6V0C*, 5′-CGCGTCCCCGTCCATCATCCCAGTGGTCTT CAAGAGAGACCACTGG GATGATGGACTTTTTGGAAAT-3′ (L), 5′-CGATTTCCAAAAAGTCC ATCATCCCAGTGGTCTCTCTTGAAGACCACTGGGATGATGGACGG GG A -3′ (R).

LENTIVIRUS PRODUCTION AND TRANSDUCTION

Virus packaging was performed in HEK 293T cells after the cotransfection of pWPXL-*CERS2*, pLVTHM-shRNA-*CERS2* or pLVTHM-shRNA-*ATP6V0C* with the packaging plasmid psPAX2 (Addgene plasmid 12260, Didier Trono) and the envelope plasmid pMD2.G (Addgene plasmid 12259, Didier Trono) using Lipofect-amine 2000 (Invitrogen, Carlsbad, CA). Viruses were harvested 48 h after transfection. Target cells were infected with filtered lentivirus in the presence of 6 μg/ml polybrene (Sigma–Aldrich, St. Louis, MO) [Ding et al., 2010].

PROTEIN EXTRACTION AND WESTERN BLOTTING

Total protein was extracted from the homogenate of cells using the T-PER Tissue Protein Extraction Reagent (Thermo Scientific, #78510). The plasma membrane protein was collected by using a plasma membrane protein extraction kit (Abcam Inc., ab65400). The proteins were separated by SDS–PAGE and transferred to nitro-cellulose membrane (Bio-Rad, Hercules, CA). The membrane was blocked with 5% non-fat milk and incubated with mouse anti-CERS2 polyclonal antibody (pAb) (Abnova Corporation) (1:1000), mouse anti-ATP6V0C pAb (Abcam Inc.) (1:1000), mouse anti-MMP-2 mAb (Chemicon) (1:1000), rabbit anti-MMP-9 pAb (Cell Signaling Technology) (1:1000), rabbit anti-TIMP1 (Cell Signaling Technol-ogy) (1:1000), rabbit anti-TIMP2 (Cell Signaling Technology) (1:1000), mouse anti-Na/K ATPase α1 mAb (Novus Biologicals) (1:1000) or rabbit anti-β-actin pAb (Bioworld Technology) (1:5000). The proteins were detected with enhanced chemiluminescence reagents (Pierce).

RTCA INVASION ASSAY

RTCA (real-time cell analyzer) invasion assay measures the effect of any perturbations in a label-free real-time setting. As cell invade from the upper chamber through the membrane into the bottom chamber in response to a chemoattractant, they contact and adhere to the electronic sensors on the underside of the membrane, resulting in an increase in the electrical impedance. The increase in the impedance correlates with increasing numbers of invaded cells on the underside of the membrane [Dunne et al., 2014; Jurmeister et al., 2012].

For the RTCA invasion assay, the upper side of the membrane was covered with a layer of Matrigel. The Matrigel (Catalog Number: 356234, Protein Concentration: 8.95 mg/ml, BD Bio-sciences, MA) was thawed overnight at 4°C and diluted 1:40 with ice-cold serum-free medium. All materials used to handle the Matrigel (pipet tips, CIM-Plates 16) were precooled overnight. Preparation of a Matrigel layer on the CIM-Plate 16 upper chamber membranes was carried out by adding 50 μl of the dilution sequentially on top of the membranes followed by immediate removal of 30 μl, leaving a total of 20 μl Matrigel dilution. The coated membranes in the upper chambers were then incubated at 37°C for 4 h to ensure homogeneous gelification followed by the addition of 165 μl (containing 10% FBS) and 30 μl (serum-free) of medium to the lower and upper chambers, respectively. Then, the CIM-Plate 16 was locked in the RTCA DP device at 37°C and 5% CO_2 for 1 h to equilibrate the medium. At the end of the incubation period, a measurement step was performed as background signal generated by cell-free media. To begin an experiment, cells were prepared in serum-free medium at the concentration of 4×10^5 cells/ml. Add 100 μl cell suspension to the upper chamber. After cell addition, CIM-Plate 16 remained at room temperature in the laminar flow hood for 30 min. Each condition was performed with a programmed signal detection every 15 min for a total 48 h. Data acquisition and analysis was performed with the RTCA software (version 2.0, Roche Diagnostics).

TRANSWELL MIGRATION AND INVASION ASSAYS

For the transwell migration assay, 5×10^4 cells were placed on the top chamber of each insert (BD Biosciences, NJ) with the noncoated membrane. For the invasion assay, 1×10^5 cells were placed on the upper chamber of each insert coated with 150 μg Matrigel (BD Biosciences, MA). Cells in both assays were trypsinized and resuspended in DMEM, and 700–900 μl of medium supplemented with 10% fetal bovine serum was injected into the lower chambers. After several hours of incubation at 37°C, any cells remaining in the top chambers or on the upper membrane of the inserts were carefully removed. After fixation and staining in a dye solution containing 0.1% crystal violet and 20% methanol, cells adhering to the lower membrane of the inserts were counted and imaged through a Leica DMI4000B inverted fluorescence (Leica, Wetzlar, Germany).

SCRATCH–WOUND ASSAY

Scratch-wound assay was conducted as previously described by us [Fan et al., 2013]. The migration of cells into the wound was monitored in multiple wells using a CellVoyager CV1000 confocal scanner system (Yokogawa Electronic, Tokyo, Japan) with an Olympus UPLSApo 10 × 2 10 × /0.4 Dry ∞/0.17/26.5 WD 3.1 plan super apochromat objective lens. The images were acquired every 0.5 h for 46 h (or every 0.5 h for 32 h). The images shown represent 0 and 46 h (or 0 and 32 h).

REVERSE TRANSCRIPTION AND QUANTITATIVE REAL–TIME PCR

Total RNA was isolated from cells with the TRIzol reagent (Invitrogen) according to the manufacturer's protocol. Real-time polymerase chain reaction was performed with the StepOne Plus sequence detection system (Applied Biosystems, Foster City, CA). The *CERS2* primers for the SYBR Green assay (Takara, Dalian, China) were: 5′-GCCCAAGCAGGTGGAAGTAGAG-3′ (L), 5′-CCAGGGTTTA TCCACAATGACG-3′ (R). The *ATP6V0C* primers were: 5′-TGCTTCGTTTTTCGCCGTCA-3′ (L), 5′-GCCACCAC-CAGGCCGTAGAT-3′ (R). The β-*actin* primers were: 5′-TTGTTA-CAGGAAGTCCCTTGCC-3′ (L), 5′-ATGCTATCACCTCCCCTGTGTG-3′ (R).
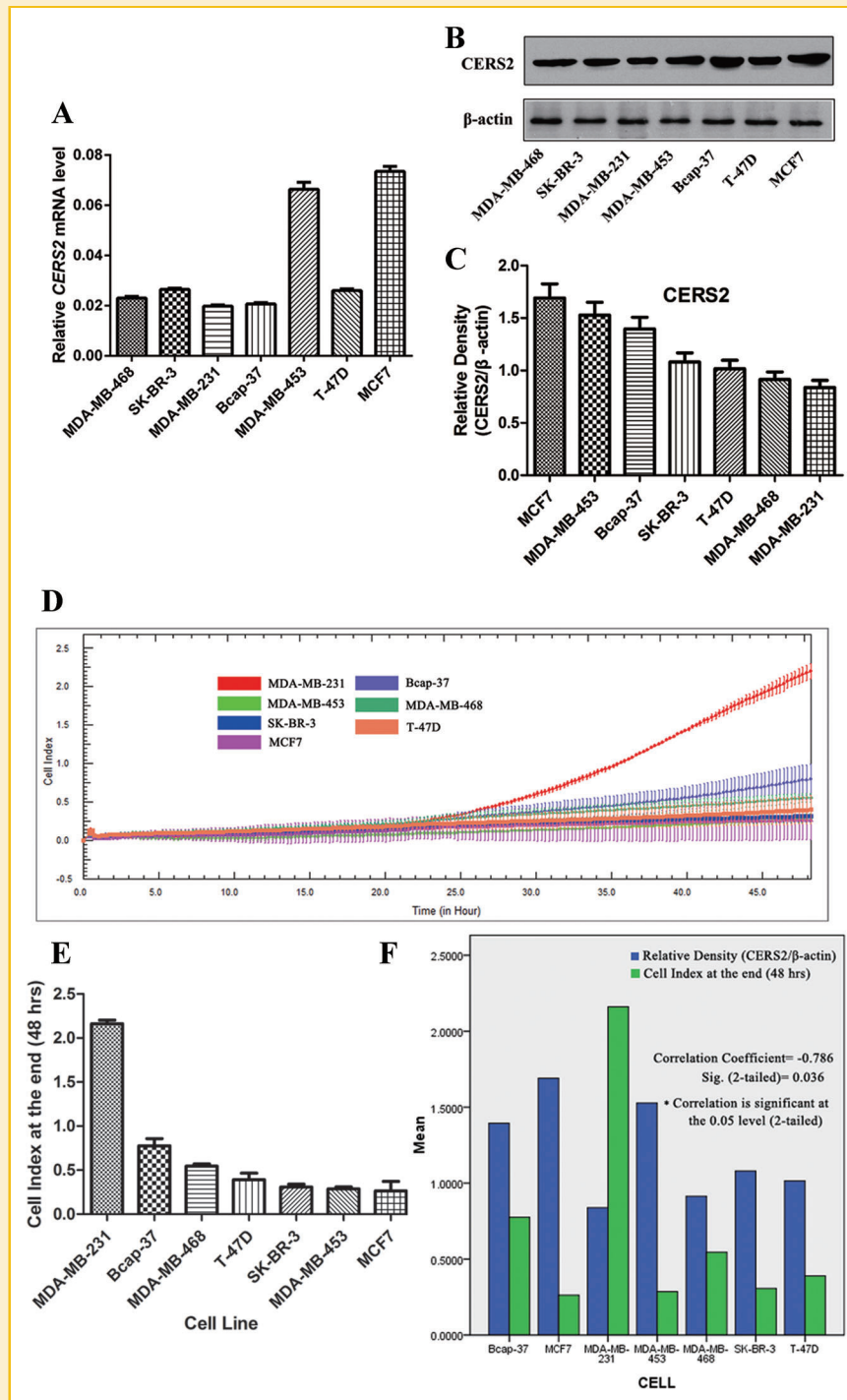
Fig. 1. Association between CERS2 expression and tumor invasion in breast cancer cell lines. The expression levels of CERS2 in various breast cancer cell lines were determined by quantitative Real-time PCR (A) and Western Blotting (B). (C) Relative density analysis of the CERS2 protein bands. The relative density is expressed as the ratio CERS2/β-actin. (D) Real time invasion analysis of seven breast cancer cell lines. The methods were described in MATERIALS and METHODS. Invasion was monitored for 48 h in the xCELLigence DP system. The cell index was measured every 15 min. The rate of change of cell index as a function of time was calculated as a measure of invasive activity. (E) The cell index at the end (48 h) is shown as a bar chart. (F) Association between CERS2 expression and tumor invasion in seven breast cancer cell lines (Correlation Coefficient = –0.786, Correlation is significant at the 0.05 level).

ACTIVITY OF V-ATPASE

Assays were performed as described previously by [2013] and us [Fan et al., 2013].

MEASUREMENT OF EXTRACELLULAR PH

Assays were performed as described previously by us [Fan et al., 2013]. Extracellular pH (pH_e) was measured using the pH-sensitive dye 2′,7′-Bis(2-carboxyethyl)-5(6)-carboxyfluorescein (BCECF) (Sigma–Aldrich, St. Louis, MO). The proton secretion ability was determined by measuring pH_e. Cells (1×10^4/well) were seeded in a 96-well plate and cultured in standard DMEM medium (pH 7.0) containing 5% FBS at 37°C in 5% CO_2 for 5 h. The medium was removed after the cells attached to the plate. The cells were washed twice using 0.9% NaCl, and were incubated with 120 μl serum-free HCO_3^--buffered DMEM medium [1 mmol/L NaHCO₃ (pH 7.0)]. After the cells were cultured for 3, 6, or 9 h, 100 μl supernatant per well was collected and 1 μmol/l BCECF was added into each sample. The sample was excited at 490 and 440 nm and the emitted fluorescence was measured at 535 nm by the luminescence spectrometer. pH_e was calibrated with the curve plotted by the fluorescence ratio *F490/F440* of the DMEM medium containing 1 μmol/L BCECF with a series of pH values buffered by HCO_3^- (1 mmol/L NaHCO₃). The pH_e value was converted to the extracellular proton concentration.

TOTAL (PRO- AND ACTIVE FORMS) AND ACTIVE FORMS OF MMP-2 AND MMP-9

Cells were seeded onto 24-well plates at a density of 1×10^5 cells per well in 500 μl culture media. These cells were cultured for two days until confluence. The supernatants from the cell culture were collected after 10 min centrifugation. Then, total and active forms of MMP-2 and MMP-9 were quantified in the culture supernatants using protein-specific Biotrak assay systems (MMP-2 Biotrak Activity Assay RPN2631; MMP-9 Biotrak Activity Assay RPN2634, GE Healthcare) according to the manufacturer's instructions. The absorbance was measured by spectrophotometry at 405 nm. The amount of total protein in the culture supernatants was measured using the Bio-Rad protein assay (Bio-Rad). Data for total and active MMP-2 and MMP-9 in the culture media were normalized against the total protein content of the culture supernatants. All experiments were performed in duplicate.

STATISTICAL ANALYSIS

Data are presented as means ± SEM and comparisons were made using Student's *t* test. A probability of 0.05 or less was considered statistically significant.
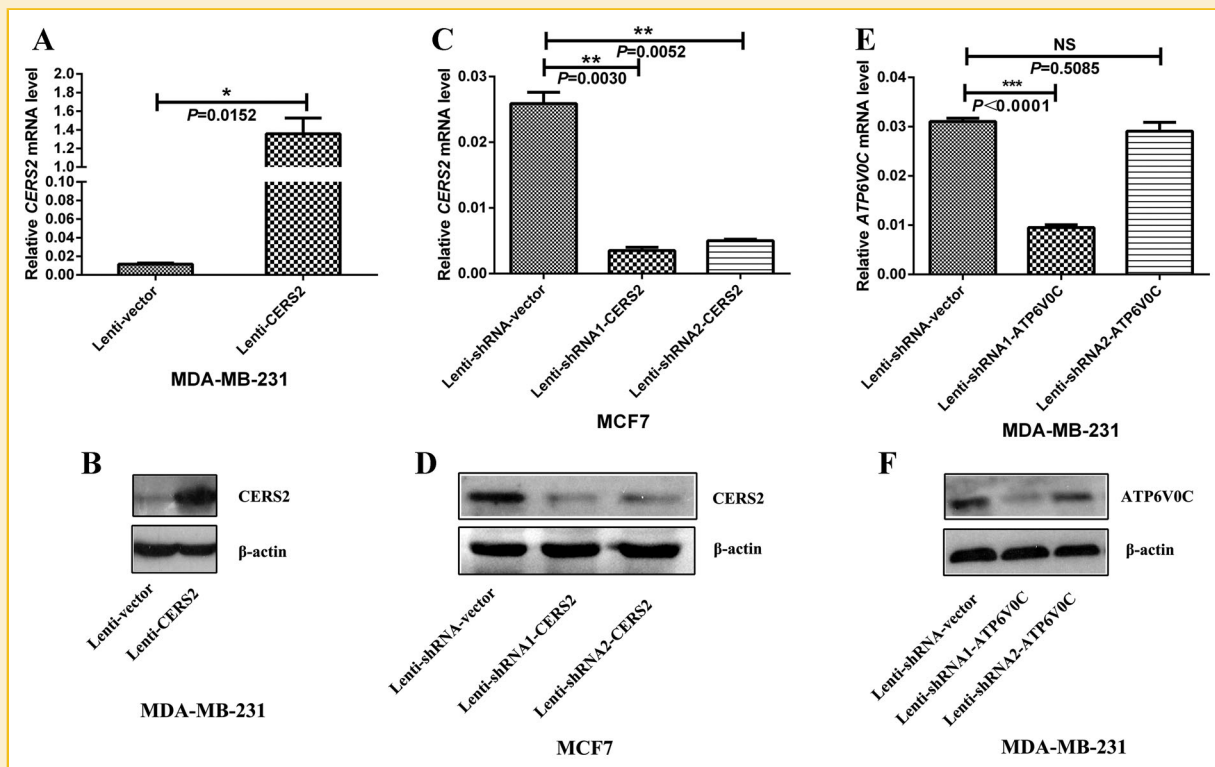

Fig. 2. Establishment of stably transfected cell lines. Real time quantitative PCR (A) and western blot (B) analyses of CERS2 expression in the CERS2 over–expression cell lines derived from MDA–MB–231 cells. Real time quantitative PCR (C) and western blot (D) analyses of CERS2 expression in the CERS2 knock–down cell lines derived from MCF7 cells. Real time quantitative PCR (E) and western blot (F) analyses of ATP6V0C expression in the CERS2 knock–down cell lines derived from MDA–MB–231 cells. The values shown are expressed as the mean ± S.E.M. Lenti–vector, the vector control cell line; Lenti–CERS2, CERS2 over–expression stable cell line; Lenti–shRNA–CERS2, CERS2 knockdown stable cell line; Lenti–shRNA–ATP6V0C, ATP6V0C knockdown stable cell line.

INVERSE ASSOCIATION BETWEEN CERS2 EXPRESSION AND TUMOR INVASION

To elucidate the role of CERS2 in breast cancer, we first examined the mRNA (Fig. 1A) and protein (Fig. 1B,C) expression of CERS2 in breast cancer cell lines. CERS2 was heterogeneously expressed in various breast cancer cells. MCF7 cells expressed relatively higher levels of CERS2 protein than other cells, and MDA-MB-231 cells expressed relatively lower levels of CERS2 protein (Fig. 1C). To determine if there is a correlation between CERS2 protein levels and invasive abilities in breast cancer cell lines, we then examined the invasive
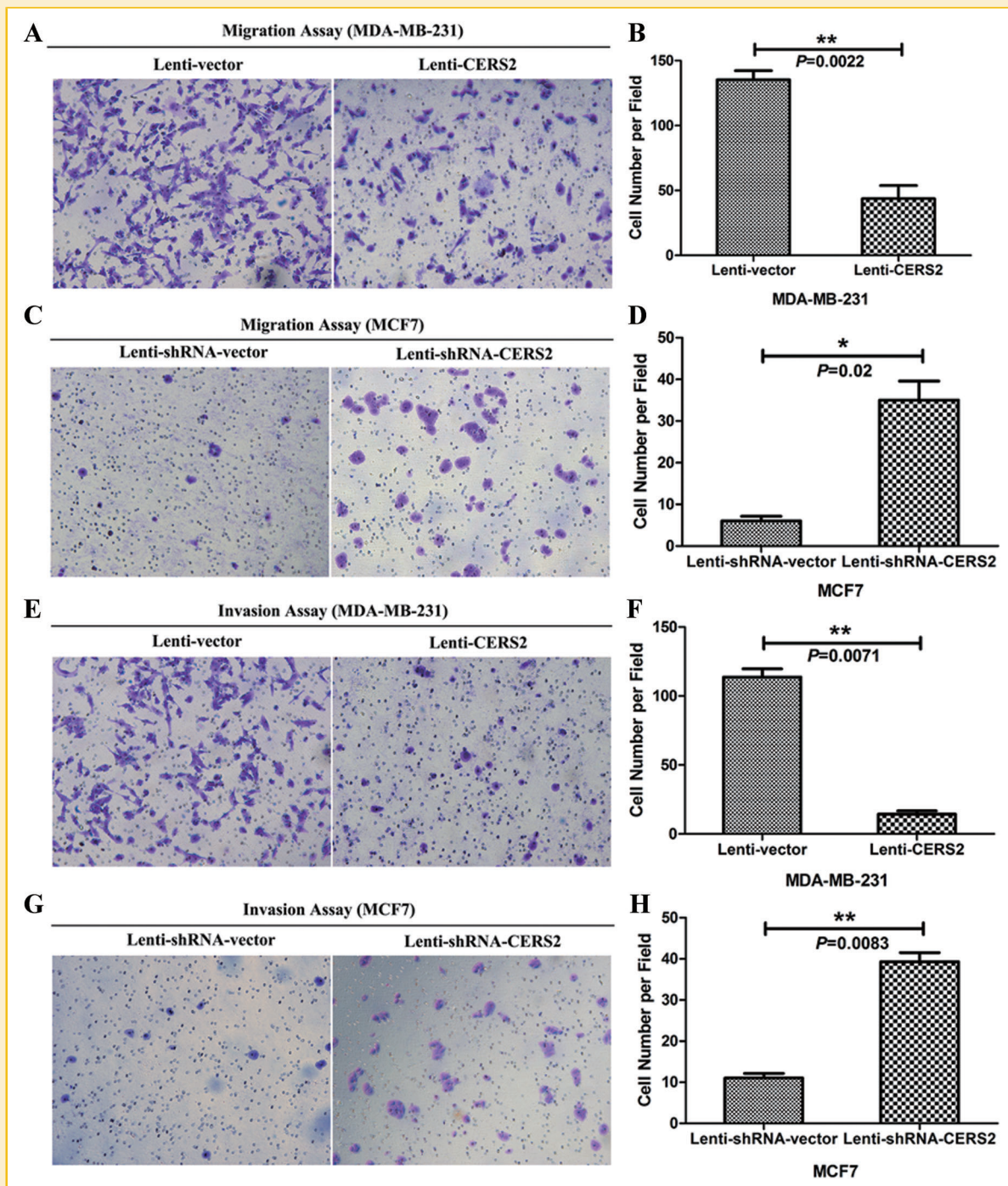

Fig. 3. CERS2 inhibited breast cancer cell migration and invasion. (A–B) The overexpression of CERS2 inhibited the migration rate of MDA–MB–231 cells. (C–D) The knockdown of CERS2 enhanced the cell migration rate of MCF7 cells. (E–F) The overexpression of CERS2 inhibited the invasion rate of MDA–MB–231 cells. (G–H) The knockdown of CERS2 enhanced the cell invasion rate of MCF7 cells.

ability of these cell lines using the RTCA xCELLigence system. Results showed that MCF7 cells are poorly invasive, and MDA-MB-231 cells are highly invasive (Fig. 1D,E). These results are consistent with other reports [Phromnoi et al., 2009; Capecci and Forgac, 2013]. Intriguingly, across all cell lines tested, we found a significant inverse correlation between CERS2 protein levels and invasive abilities (Correlation Coefficient = -0.786, $P = 0.036$; Fig. 1F). We chose the relatively CERS2-highly-expressed cell line MCF7 (poorly invasive breast cancer cells) and the relatively CERS2-lowly-expressed cell line MDA-MB-231 (highly invasive breast cancer cells) for functional investigation.

ESTABLISHMENT OF STABLY TRANSFECTED CELL LINES

We established stable cell lines transduced by a lentivirus carrying the *CERS2* gene or no insert (vector control), which were designated as Lenti-CERS2 and Lenti-vector, respectively, in the breast cancer cell line MDA-MB-231 (Fig. 2A,B). Furthermore, we established stable cell lines transduced by a lentivirus carrying *CERS2*-short hairpin RNA (shRNA), which were designated as Lenti-shRNA-CERS2, in the breast cancer cell line MCF7 (Fig. 2C,D). MDA-MB-231 cells express much higher levels of V-ATPase at the plasma membrane than poorly invasive MCF7 cells [Sennoune et al., 2004]. We also established stable cell lines transduced by a lentivirus carrying *ATP6V0C*-short hairpin RNA, which were designated as Lenti-shRNA-ATP6V0C, in the breast cancer cell line MDA-MB-231 (Fig. 2E,F). Real-time PCR (Fig. 2C) and Western blotting (Fig. 2D) data showed CERS2 shRNA1 was more efficient than CERS2 shRNA2. Thus, the cells infected with *CERS2* shRNA1 were used for further experiments. Our results (Fig. 2E,F) also showed *ATP6V0C* shRNA1 was more efficient than *ATP6V0C* shRNA2. So, the cells infected with *ATP6V0C* shRNA1 were used for further experiments.

EFFECT OF CERS2 ON BREAST CANCER MIGRATION AND INVASION

Transwell assays without Matrigel demonstrated that overexpression of CERS2 could significantly inhibit migration of MDA-MB-231 cells when compared with vector groups ($P = 0.0022$; Fig. 3A,B), and CERS2 knockdown in MCF7 cells significantly increased the migration capacity ($P = 0.02$; Fig. 3C,D). Transwell assays with Matrigel showed that overexpression of CERS2 could significantly inhibit the invasive capacity of MDA-MB-231 cells when compared with the control cells ($P = 0.0071$; Fig. 3E,F), and CERS2 knockdown in MCF7 cells significantly increased the invasion capacity ($P = 0.0083$; Fig. 3G,H). To further confirm this observation, we also determined the migration ability of breast cancer cells in the condition of CERS2 overexpression using a confocal scanner system. The results showed that CERS2 significantly decreased the migration of MDA-MB-231 cells compared with the vector groups (Mov. S1,2; Fig. 4A–D). In previous study, we reported that CERS2 could enhance the chemosensitivity in breast cancer cells by inhibiting the V-ATPase activity through binding to ATP6V0C [Fan et al., 2013]. In this study, we found ATP6V0C knockdown significantly decreased the migration ability of MDA-MB-231 cells compared with the vector groups (Mov. S3,4; Fig. 4E–H).

INHIBITION OF V-ATPASE ACTIVITY

To explore whether CERS2 suppress breast cancer cell migration and invasion by inhibiting the V-ATPase activity through binding to
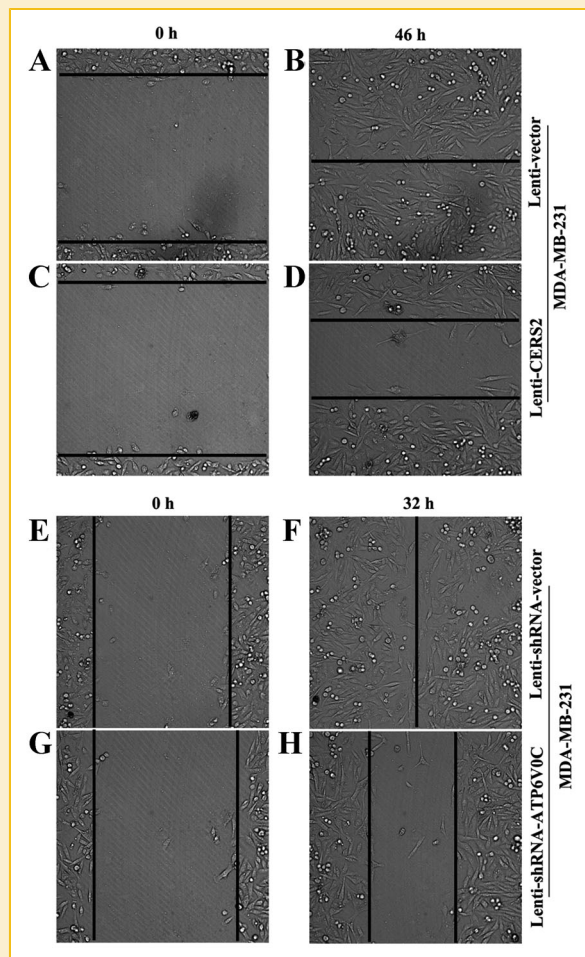

Fig. 4. The overexpression of CERS2 or knockdown of ATP6V0C inhibited migration in MDA-MB-231 cells. The migration of cells into the wound was monitored in multiple wells using a CellVoyager CV1000 confocal scanner system. The images were acquired every 0.5 h for 46 h (see Mov. S1,2) or 32 h (see Mov. S3,4). The images shown represent 0 h (Fig. 4A,C) and 46 h (Fig. 4B, D). The distance between the two edges of the scratch in the Lenti–CERS2 well (Fig. 4D) was obviously greater than that of the control (Fig. 4B). The images shown represent 0 h (Fig. 4E,G) and 32 h (Fig. 4F,H). The distance between the two edges of the scratch in the Lenti–shRNA-ATP6V0C well (Fig. 4H) was obviously greater than that of the control (Fig. 4F).

ATP6V0C, we examined the influence of CERS2 on the V-ATPase activity. Overexpression of CERS2 in MDA-MB-231 cells significantly reduced the V-ATPase activity ($P = 0.0229$; Fig. 5A), and CERS2 knockdown in MCF7 cells significantly increased the V-ATPase activity ($P = 0.0339$; Fig. 5A). V-ATPases are involved in maintaining a relatively neutral intracellular pH and an acidic extracellular pH, through pumping protons into extracellular environment [Fais et al., 2007]. In this study, the process of proton extrusion was investigated by detecting the proton concentration in the medium with pH-sensitive BCECF. As shown in Figure 5B–D, the proton secretion of MDA-MB-231-Lenti-CERS2 was notably reduced at 9 h compared with that of MDA-MB-231-Lenti-vector cells ($P = 0.0041$). Furthermore, the proton secretion of MCF7-
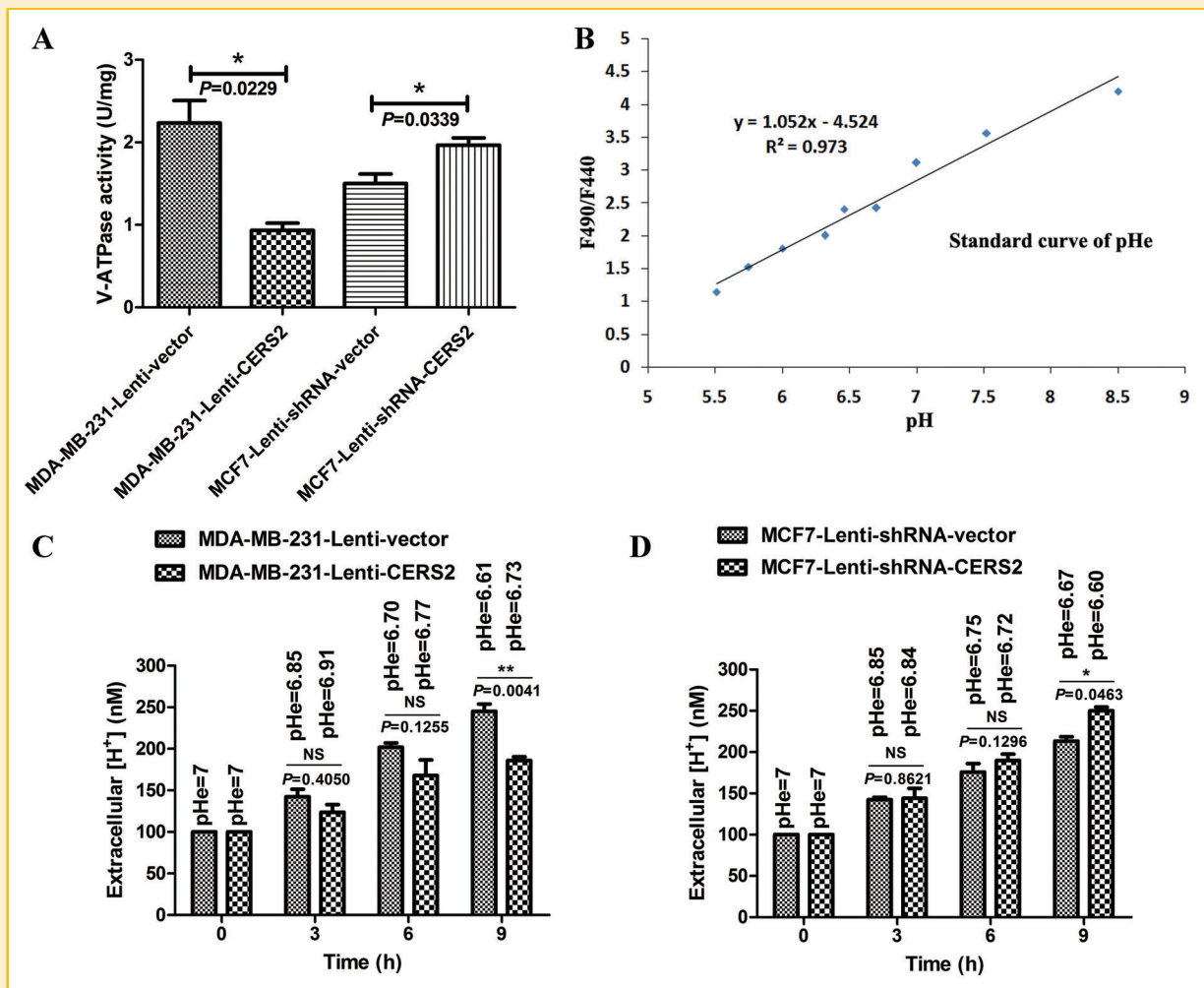
Fig. 5. Evaluation of V–ATPase activity and extracellular pH (pH$_e$). (A) Activity of V–ATPase in Lenti–CERS2 and Lenti–shRNA–CERS2 cells. (B) The standard curve for pH$_e$ assay. (C) Proton secretion was decreased in the Lenti–CERS2 cells compared with the Lenti–vector. (D) Proton secretion was increased in the Lenti–shRNA–CERS2 cells compared with the Lenti–shRNA–vector.

Lenti-shRNA-CERS2 was significantly increased compared with that of MCF7-Lenti-shRNA-vector cells ($P = 0.0463$).

EFFECT OF CERS2 ON THE ACTIVITIES OF MMP-2 AND MMP-9

The V-ATPase is the primary regulator of the tumor microenvironment, by means of proton extrusion to the extracellular medium. The acid medium confers an optimum pH to the degradative enzymes, such as matrix metalloproteinases (MMPs), for their proper function [Pérez-Sayáns et al., 2009]. The migration and invasion processes require extensive remodeling of the ECM by MMPs [Egeblad and Werb, 2002; Kummer et al., 2012]. We determined the expression levels and activities of MMP-2 and MMP-9, which are closely related to cancer invasion and metastasis according to the previous reports [Lu et al., 2005; Fagan-Solis et al., 2013]. Western blot showed that overexpression or knockdown of CERS2 didn't have obvious impacts on the protein expression levels of total MMP-2 and MMP-9 in the cells (Fig. 6A).

Results showed that overexpression or knockdown of CERS2 didn't have obvious impacts on the protein expression levels of pro-MMP-2, active MMP-2, pro-MMP-9 and active MMP-9 in the cells (Fig. S1). The supernatant of cultured cells was collected and the levels of MMP-2 and MMP-9 were assayed with MMP-2/MMP-9 Activity Assay kit. Results indicated that overexpression or knockdown of CERS2 didn't have obvious impacts on the total levels of MMP-2 and MM-9 (pro- and active MMP-2 and MMP-9) in the supernatant of cultured cells (Fig. 6B,C). Intriguingly, overexpression of CERS2 in the MDA-MB-231 cells could significantly decrease the active MMP-2 level in the supernatant of cultured cells ($P = 0.0035$; Fig. 6D). Knockdown of CERS2 in the MCF7 cells could significantly increase the active MMP-2 level in the supernatant of cultured cells ($P = 0.0057$; Fig. 6D). Our results also showed overexpression of CERS2 in the MDA-MB-231 cells could significantly decrease the active MMP-9 level in the supernatant of cultured cells ($P = 0.0078$; Fig. 6E). Knockdown of CERS2 in the
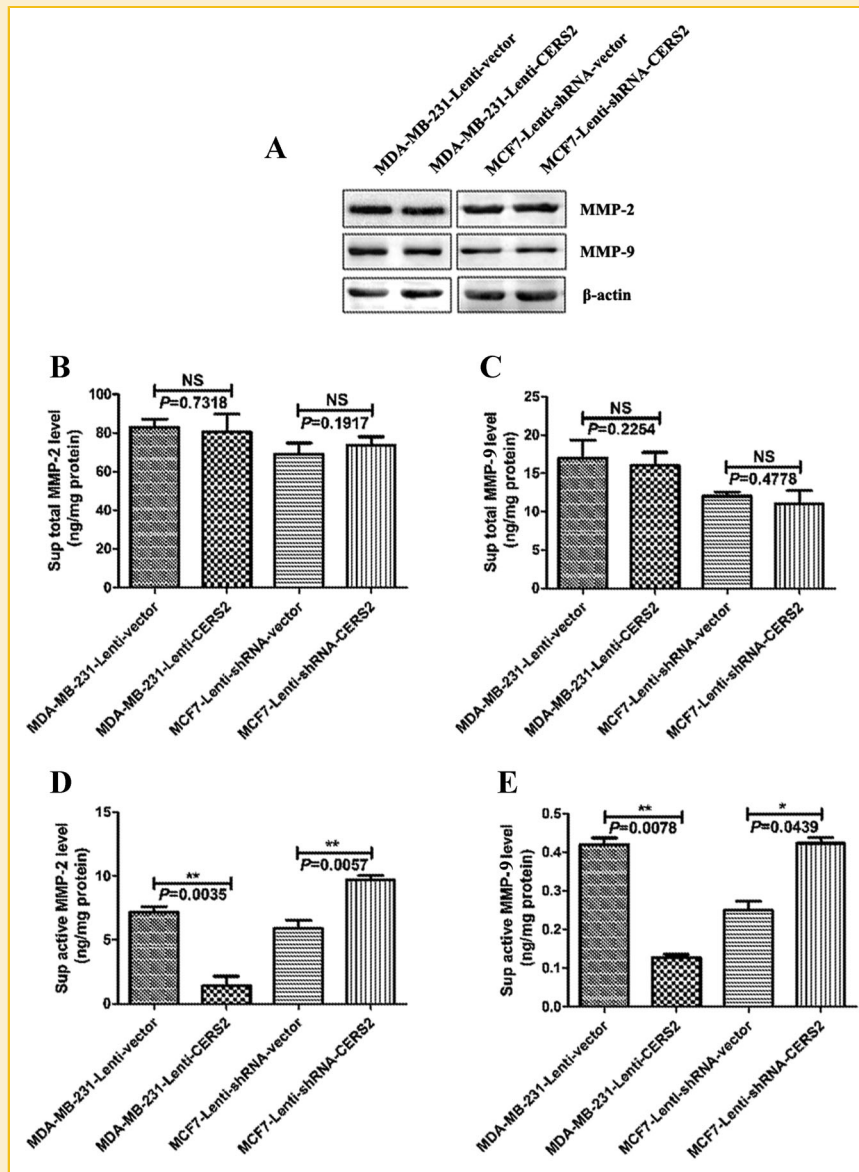
Fig. 6. Detection of MMP–2 and MMP–9 proteins. (A) The protein expression levels of MMP–2 and MMP–9 were determined by western blot assays in MDA–MB–231 and MCF7 cells after infection with CERS2, shRNA–CERS2, or respective control lentivirus. Total MMP–2 (B), total MMP–9 (C), active MMP–2 (D) and active MMP–9 (E) levels in culture supernatants were measured using the enzyme–linked immunosorbent assay (ELISA).

MCF7 cells could significantly increase the active MMP-9 level in the supernatant of cultured cells ($P = 0.0439$; Fig. 6E). These results showed that CERS2 didn't have obvious effects on the protein expression levels of MMP-2 and MMP-9 in the cells or in the supernatant, however, CERS2 have significant effects on the active MMP-2 and MMP-9 levels in the supernatant.

DISCUSSION

Our previous studies have shown that higher expression of CERS2 in the breast cancer patients was associated with fewer lymph node metastases [Wang et al., 2013]. But the molecular

mechanism is unknown. In this study, we found CERS2 was heterogeneously expressed in various breast cancer cells. The mRNA and protein expression levels of CERS2 in MCF7 cells, which are poorly invasive breast cancer cells, were obviously higher than that in the highly invasive cells MDA-MB-231. Furthermore, we found there is a inverse correlation between CERS2 protein levels and invasive abilities in breast cancer cell lines (Fig. 1). Overexpression of CERS2 in MDA-MB-231 cells (Fig. 2A,B) could significantly inhibit the migration and invasion abilities when compared with vector groups (Fig. 3A, B,E,F; Fig. 4A–D; Mov. S1,2). Conversely, CERS2 knock-down in MCF7 cells (Fig. 2C,D) could significantly increase the migration and invasion abilities (Fig. 3C,D,G,H). These results indicate that

CERS2 is involved in the migration and invasion of breast cancer cells.

An acidic microenvironment can increase tumor malignancy by promoting cell invasion [Fogarty et al., 2013]. Among the key regulators of the acidic tumor microenvironment, V-ATPases play an important role [Fan et al., 2013]. V-ATPases have been proposed as promising molecular targets for cancer invasion and metastasis [Capecci and Forgac, 2013; Fogarty et al., 2013; Hendrix et al., 2013]. Several V-ATPase inhibitors have been reported to inhibit cancer cell invasion and metastasis [Niikura 2007; Michel et al., 2013].

Studies have shown that CERS2 could interact with VPL, also called ATP6V0C or ATP6L, the c subunit of V-ATPase proton pump [Pan et al., 2001; Yu et al., 2013]. In this study, we found that inhibition of V-ATPase activity by knocking down ATP6V0C expression in MDA-MB-231 cells (Fig. 2E,F) could significantly inhibit the migration abilities of the cells (Fig. 4E,H; Mov. S3,4). To explore whether CERS2 suppresses the tumor cell migration and invasion through inhibiting the activity of V-ATPase, we examined the influence of CERS2 on the V-ATPase activity. Overexpression of CERS2 in MDA-MB-231 cells significantly reduced the V-ATPase activity (Fig. 5A), and CERS2 knockdown in MCF7 cells significantly increased the V-ATPase activity (Fig. 5A). Furthermore, we examined the influence of CERS2 on the pH_e. The results showed that overexpression of CERS2 could increase the pH_e (Fig. 5C), while knockdown of CERS2 could decrease the pH_e (Fig. 5D). These results indicate that pH_e in tumor microenvironment are raised because CERS2 inhibits the activity of V-ATPase proton pump by binding to ATP6V0C (c subunit of V-ATPase complex, providing proton a hydrophilic path across the membrane). In addition, results showed that overexpression or knockdown of CERS2 didn't have obvious impact on the protein expression levels of ATP6V0C in the cells (Fig. S2).

The promoting effect of V-ATPase on cancer invasion mainly relies on its maintain acidic pH of extracellular microenvironment, which is related to the activation, secretion, and cellular distribution of many proteases involved in the digestion of ECM [Lu et al., 2005]. The pH-sensitive proteases include cathepsin (cathepsin B, D, etc.) and MMPs (MMP-2, MMP-9, MMP-3, etc.) [Lu et al., 2005; de Lucca Camargo et al., 2013]. Our results showed that ATP6V0C knockdown in invasive MDA-MB-231 cells was associated with decreased activities of MMP-2 and MMP-9 (Fig. S3). In addition, results showed that CERS2 didn't have obvious impacts on the protein expression levels of MMP-2 and MMP-9 in the cells (Fig. 6A). Furthermore, CERS2 didn't have obvious impacts on the total levels of MMP-2 and MM-9 (pro- and active MMP-2 and MMP-9) in the supernatant of cultured cells (Fig. 6B,C). Intriguingly, CERS2 overexpression in invasive MDA-MB-231 cells is associated with decreased activities of MMP-2 and MMP-9, whereas suppression of CERS2 had the opposite effects on MMPs in non-invasive MCF7 cells (Fig. 6D,E).

In addition, some researchers have found the levels of ceramide ($C_{18:0}$-Cer, $C_{20:0}$-Cer) were significantly higher in estrogen receptor (ER) positive breast cancer tissues as compared with ER negative breast tissue samples [Schiffmann et al., 2009]. Furthermore, it is reported the expression levels of CERS4 and CERS6 are also ER status dependently regulated in breast cancer tissues [Ruckhäberle et al., 2008]. In the present study, the mRNA and protein expression levels of CERS2 in MCF7 cells were obviously higher than that in MDA-MB-231 cells. MCF7 cells are ER-positive cell line (ERα/ERβ) and MDA-MB-231 cells (ERβ) are ER-negative cell line [Pons et al., 2014]. So maybe different ER
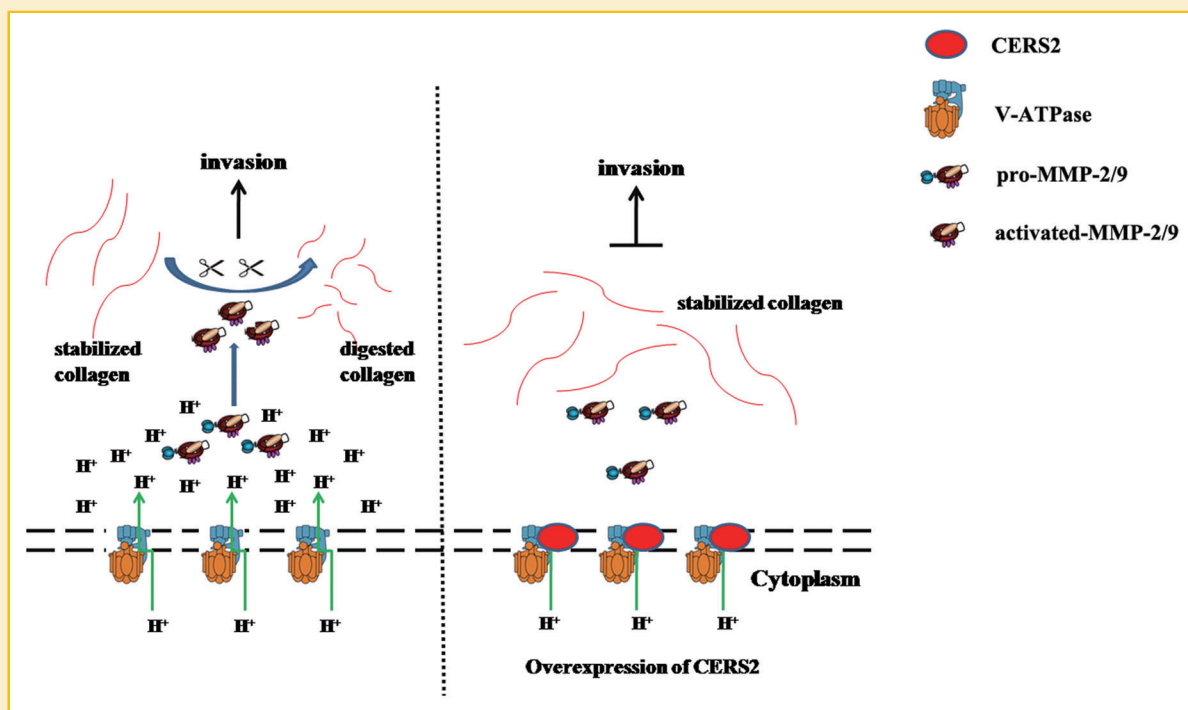

Fig. 7. A hypothetical cascade pathway of the suppression of tumor cell invasion by CERS2.

status is the most fundamental reason for the effects encountered in this study. Further studies are needed to explore this assumption.

In summary, we demonstrated that CERS2 can significantly inhibit breast cancer cell invasion and is associated with the decrease of the V-ATPase activity and extracellular hydrogen ion concentration, and in turn the activation of secreted MMP-2/MMP-9 and degradation of ECM, which ultimately suppressed tumor's invasion (Fig. 7), indicating that CERS2 may be a novel invasion suppressor gene.

REFERENCES

Capecci J, Forgac M. 2013. The function of vacuolar ATPase (V-ATPase) a subunit isoforms in invasiveness of MCF10a and MCF10CA1a human breast cancer cells. J Biol Chem 288:32731–32741.

Cardoso AP, Pinto ML, Pinto AT, Oliveira MI, Pinto MT, Gonçalves R, Relvas JB, Figueiredo C, Seruca R, Mantovani A, Mareel M, Barbosa MA, Oliveira MJ. 2014. Macrophages stimulate gastric and colorectal cancer invasion through EGFR Y1086, c-Src, Erk1/2 and Akt phosphorylation and smallGTPase activity. Oncogene 33:2123–2133.

Chung C, Mader CC, Schmitz JC, Atladottir J, Fitchev P, Cornwell ML, Koleske AJ, Crawford SE, Gorelick F. 2011. The vacuolar-ATPase modulates matrix metalloproteinase isoforms in human pancreatic cancer. Lab Invest 91:732–743.

Cruciat CM, Ohkawara B, Acebron SP, Karaulanov E, Reinhard C, Ingelfinger D, Boutros M, Niehrs C. 2010. Requirement of prorenin receptor and vacuolar H$^+$-ATPase-mediated acidification for Wnt signaling. Science 327:459–463.

de Lucca Camargo L, Babelova A, Mieth A, Weigert A, Mooz J, Rajalingam K, Heide H, Wittig I, Lopes LR, Brandes RP. 2013. Endo-PDI is required for TNFα-induced angiogenesis. Free Radic Biol Med 65:1398–1407.

Ding J, Huang S, Wu S, Zhao Y, Liang L, Yan M, Ge C, Yao J, Chen T, Wan D, Wang H, Gu J, Yao M, Li J, Tu H, He X. 2010. Gain of miR-151 on chromosome 8q24.3 facilitates tumour cell migration and spreading through downregulating RhoGDIA. Nat Cell Biol 12:390–399.

Dunne PD, McArt DG, Blayney JK, Kalimutho M, Greer S, Wang T, Srivastava S, Ong CW, Arthur K, Loughrey M, Redmond K, Longley DB, Salto-Tellez M, Johnston PG, Van Schaeybroeck S. 2014. AXL is a key regulator of inherent and chemotherapy-induced invasion and predicts a poor clinical outcome in early-stage colon cancer. Clin Cancer Res 20:164–175.

Egeblad M, Werb Z. 2002. New functions for the matrix metalloproteinases in cancer progression. Nat Rev Cancer 2:161–174.

Erez-Roman R, Pienik R, Futerman AH. 2010. Increased ceramide synthase 2 and 6 mRNA levels in breast cancer tissues and correlation with sphingosine kinase expression. Biochem Biophys Res Commun 391:219–223.

Fagan-Solis KD, Schneider SS, Pentecost BT, Bentley BA, Otis CN, Gierthy JF, Arcaro KF. 2013. The RhoA pathway mediates MMP-2 and MMP-9-independent invasive behavior in a triple-negative breast cancer cell line. J Cell Biochem 114:1385–1394.

Fais S, De Milito A, You H, Qin W. 2007. Targeting vacuolar H$^+$-ATPase as a new strategy against cancer. Cancer Res 67:10627–10630.

Fan S, Niu Y, Tan N, Wu Z, Wang Y, You H, Ke R, Song J, Shen Q, Wang W, Yao G, Shu H, Lin H, Yao M, Zhang Z, Gu J, Qin W. 2013. LASS2 enhances chemosensitivity of breast cancer by counteracting acidic tumor microenvironment through inhibiting activity of V-ATPase proton pump. Oncogene 32:1682–1690.

Fang M, Yuan JP, Peng CW, Pang DW, Li Y. 2013. Quantum dots-based *in situ* molecular imaging of dynamic changes of collagen IV during cancer invasion. Biomaterials 34:8708–8717.

Fitzgerald S, Sheehan KM, O'Grady A, Kenny D, O'Kennedy R, Kay EW, Kijanka G. 2013. Increased ceramide synthase 5 expression is associated with lymphovascular invasion, metastasis and poor survival in colorectal cancer. Cancer Res 73(8Suppl).

Fogarty FM, O'Keeffe J, Zhadanov A, Papkovsky D, Ayllon V, O'Connor R. 2013. HRG-1 enhances cancer cell invasive potential and couples glucose metabolism to cytosolic/extracellular pH gradient regulation by the vacuolar-H$^+$ ATPase. Oncogene 1.DOI: 10.1038/onc.2013.403...[in press].

Hendrix A, Sormunen R, Westbroek W, Lambein K, Denys H, Sys G, Braems G, Van den Broecke R, Cocquyt V, Gespach C, Bracke M, De Wever O. 2013. Vacuolar H$^+$ ATPase expression and activity is required for Rab27B-dependent invasive growth and metastasis of breast cancer. Int J Cancer 133:843–854.

Jurmeister S1, Baumann M, Balwierz A, Keklikoglou I, Ward A, Uhlmann S, Zhang JD, Wiemann S, Sahin Ö. 2012. MicroRNA-200c represses migration and invasion of breast cancer cells by targeting actin-regulatory proteins FHOD1 and PPM1F. Mol Cell Biol 32:633–651.

Kessenbrock K, Plaks V, Werb Z. 2010. Matrix metalloproteinases: regulators of the tumor microenvironment. Cell 141:52–67.

Koybasi S, Senkal CE, Sundararaj K, Spassieva S, Bielawski J, Osta W, Day TA, Jiang JC, Jazwinski SM, Hannun YA, Obeid LM, Ogretmen B. 2004. Defects in cell growth regulation by C18: 0–ceramide and longevity assurance gene 1 in human head and neck squamous cell carcinomas. J Cell Biochem 279:44311–44319.

Kummer NT, Nowicki TS, Azzi JP, Reyes I, Iacob C, Xie S, Swati I, Darzynkiewicz Z, Gotlinger KH, Suslina N, Schantz S, Tiwari RK, Geliebter J. 2012. Arachidonate 5 lipoxygenase expression in papillary thyroid carcinoma promotes invasion via MMP-9 induction. J Cell Biochem 113:1998–2008.

Laviad EL, Albee L, Pankova-Kholmyansky I, Epstein S, Park H, Merrill AH, Jr, Futerman AH. 2008. Characterization of ceramide synthase 2: tissue distribution, substrate specificity, and inhibition by sphingosine 1-phosphate. J Biol Chem 283:5677–5684.

Lu P, Weaver VM, Werb Z. 2012. The extracellular matrix: A dynamic niche in cancer progression. J Cell Biol 196:395–406.

Lu X, Qin W, Li J, Tan N, Pan D, Zhang H, Xie L, Yao G, Shu H, Yao M, Wan D, Gu J, Yang S. 2005. The growth and metastasis of human hepatocellular carcinoma xenografts are inhibited by small interfering RNA targeting to the subunit ATP6L of proton pump. Cancer Res 65:6843–6849.

Michel V, Licon-Munoz Y, Trujillo K, Bisoffi M, Parra KJ. 2013. Inhibitors of vacuolar ATPase proton pumps inhibit human prostate cancer cell invasion and prostate-specific antigen expression and secretion. Int J Cancer 132:E1–10.

Niikura K. 2007. Effect of a V-ATPase inhibitor, FR202126, in syngeneic mouse model of experimental bone metastasis. Cancer Chemother Pharmacol 60:555–562.

Pan H, Qin WX, Huo KK, Wan DF, Yu Y, Xu ZG, Hu QD, Gu KT, Zhou XM, Jiang HQ, Zhang PP, Huang Y, Li YY, Gu JR. 2001. Cloning, mapping, and characterization of a human homologue of the yeast longevity assurance gene *LAG1*. Genomics 77:58–64.

Pérez-Sayáns M, García-García A, Reboiras-López MD, Gándara-Vila P. 2009. Role of V-ATPases in solid tumors: Importance of the subunit C (Review). Int J Oncol 34:1513–1520.

Phromnoi K, Yodkeeree S, Anuchapreeda S, Limtrakul P. 2009. Inhibition of MMP-3 activity and invasion of the MDA-MB-231 human invasive breast carcinoma cell line by bioflavonoids. Acta Pharmacol Sin 30: 1169–1176.

Pons DG, Nadal-Serrano M, Blanquer-Rossello MM, Sastre-Serra J, Oliver J, Roca P. 2014. Genistein modulates proliferation and mitochondrial functionality in breast cancer cells depending on ERalpha/ERbeta ratio. J Cell Biochem 115:949–958.

Rofstad EK, Mathiesen B, Kindem K, Galappathi K. 2006. Acidic extracellular pH promotes experimental metastasis of human melanoma cells in athymic nude mice. Cancer Res 66:6699–6707.

Rojas JD, Sennoune SR, Maiti D, Bakunts K, Reuveni M, Sanka SC, Martinez GM, Seftor EA, Meininger CJ, Wu G, Wesson DE, Hendrix MJ, Martínez-Zaguilán R. 2006. Vacuolar-type H$^+$-ATPases at the plasma membrane regulate pH and cell migration in microvascular endothelial cells. Am J Physiol Heart Circ Physiol 291:H1147–H1157.

Ruckhäberle E, Rody A, Engels K, Gaetje R, von Minckwitz G, Schiffmann S, Grösch S, Geissslinger G, Holtrich U, Karn T, Kaufmann M. 2008. Microarray analysis of altered sphingolipid metabolism reveals prognostic significance of sphingosine kinase 1 in breast cancer. Breast Cancer Res Treat 112:41–52.

Schiffmann S, Sandner J, Birod K, Wobst I, Angioni C, Ruckhäberle E, Kaufmann M, Ackermann H, Lötsch J, Schmidt H, Geissslinger G, Grösch S. 2009. Ceramide synthases and ceramide levels are increased in breast cancer tissue. Carcinogenesis 30:745–752.

Sennoune SR, Bakunts K, Martínez GM, Chua-Tuan JL, Kebir Y, Attaya MN, Martínez-Zaguilán R. 2004. Vacuolar H$^+$-ATPase in human breast cancer cells with distinct metastatic potential: distribution and functional activity. Am J Physiol Cell Physiol 286:C1443–C1452.

Siegel R, Naishadham D, Jemal A. 2013. Cancer statistics. CA Cancer J Clin 63:11–30.

Wang YY, Gao LY, Zhao YH, Li JY, Luo Q, Fan SH. 2013. Expression of CERS2 in invasive breast cancer tissues and its clinical significance. Zhonghua Bing Li Xue Za Zhi 42:267–268.

Wiedmann RM, von Schwarzenberg K, Palamidessi A, Schreiner L, Kubisch R, Liebl J, Schempp C, Trauner D, Vereb G, Zahler S, Wagner E, Müller R, Scita G, Vollmar AM. 2012. The V-ATPase-inhibitor archazolid abrogates tumor metastasis via inhibition of endocytic activation of the Rho-GTPase Rac1. Cancer Res 72:5976–5987.

Yu W, Wang L, Wang Y, Xu X, Zou P, Gong M, Zheng J, You J, Wang H, Mei F, Pei F. 2013. A novel tumor metastasis suppressor gene LASS2/TMSG1 interacts with vacuolar ATPase through its homeodomain 114:570–583.

SUPPORTING INFORMATION

Additional Supporting Information may be found in the online version of this article at the publisher's web-site.